MOLECULAR AND CELLULAR BIOLOGY, Feb. 2000, p. 1419–1425 Vol. 20, No. 4
0270-7306/00/$04.00+0

Minimal Phenotype of Mice Homozygous for a Null Mutation in the Forkhead/Winged Helix Gene, *Mf2*

TSUTOMU KUME,[1] KEYU DENG,[1] AND BRIGID L. M. HOGAN[2]*

Howard Hughes Medical Institute[2] and Department of Cell Biology,[1] Vanderbilt University Medical Center, Nashville, Tennessee 37232-2175

Received 11 November 1999/Accepted 17 November 1999

***Mf2* (mesoderm/mesenchyme forkhead 2) encodes a forkhead/winged helix transcription factor expressed in numerous tissues of the mouse embryo, including paraxial mesoderm, somites, branchial arches, vibrissae, developing central nervous system, and developing kidney. We have generated mice homozygous for a null mutation in the *Mf2* gene (*Mf2*^{lacZ}) to examine its role during embryonic development. The *lacZ* allele also allows monitoring of *Mf2* gene expression. Homozygous null mutants are viable and fertile and have no major developmental defects. Some mutants show renal abnormalities, including kidney hypoplasia and hydroureter, but the penetrance of this phenotype is only 40% or lower, depending on the genetic background. These data suggest that *Mf2* can play a unique role in kidney development, but there is functional redundancy in this organ and other tissues with other forkhead/winged helix genes.**

Forkhead/winged helix proteins constitute a large family of transcription factors that share an evolutionarily conserved DNA binding domain. There is now extensive evidence that these proteins are components of different signal transduction pathways and play numerous and crucial roles in embryonic development, including cell fate determination, proliferation, and differentiation (for a review, see reference 23). In the mouse, a number of forkhead genes have been identified and inactivated by homologous recombination in embryonic stem (ES) cells, providing evidence for both unique and functionally redundant roles in development (1, 4, 22, 25, 26, 42, 45).

Our laboratory has previously identified and focused on four murine forkhead/winged helix genes that are all expressed in, among other tissues, the paraxial mesoderm and early somites of the mouse embryo (36). These are *Mf1* (*mesoderm/mesenchyme forkhead 1*), *Mf2*, *Mf3* (also known as *fkh5*, *hfh-e5.1*, and *twh*), and *Mfh1* (*mesenchyme forkhead 1*) (2, 6, 21, 30). Homozygous null *Mf3* mutant mice have numerous abnormalities, including perinatal mortality, growth retardation, nursing defects, and defects of the central nervous system (CNS) (6, 26, 41). The CNS abnormalities relate to *Mf3* expression in specific cell populations of the developing hypothalamus and spinal cord. However, the mutant mice have no obvious defects in somites or their derivatives, suggesting functional redundancy in mesodermal tissues with other forkhead genes such as *Mf1*, *Mfh1*, and *Mf2*. *Mf1* and *Mfh1* encode proteins with virtually identical DNA binding domains and distinct but overlapping expression patterns during embryonic development (17, 19, 25, 30, 36, 39, 42, 43). *Mf1*^{lacZ} homozygotes die pre- and perinatally with multiple abnormalities, including hemorrhagic hydrocephalus and skeletal, ocular, and cardiovascular defects (24, 25, 43). Identical developmental abnormalities are seen in the spontaneous *congenital hydrocephalus* (now *Mf1*^{ch}) mutant, which we have shown to be an allele of *Mf1* (15, 18, 25). Homozygous *Mfh1*^{tm1} null mutants also die pre- or perinatally with defects in the skull, axial skeleton, and cardiovascular system (19, 42). The skeletal defects in *Mfh1* null mutants are different from those seen in *Mf1*^{lacZ} and *Mf1*^{ch} mutants. However, the cardiovascular defects are similar, and in addition, the majority of embryos that are doubly heterozygous for mutations in *Mf1*^{lacZ} and *Mfh1*^{tm1} die prenatally with the same spectrum of cardiovascular abnormalities as each single homozygous mutant (43). These results provide evidence for nonallelic noncomplementation between *Mf1* and *Mfh1* and suggest cooperative interaction between the two genes in tissues such as those of the developing cardiovascular system.

We focus here on the *Mf2* gene, which encodes a protein with a DNA binding domain virtually identical to that of brain factor 2 (Bf2). *Mf2* is expressed in the paraxial mesoderm in the early mouse embryo, and somite expression of *Mf2* overlaps that of *Mf1*, *Mfh1*, and *Mf3* (36, 44). In addition, the *Mf2* and *Bf2* genes have overlapping expression patterns in other tissues, including the tongue, meninges, mesenchyme of the vibrissae, and metanephric kidney (16, 44).

To examine the role of *Mf2* during development, we generated homozygous null mutants (*Mf2*^{lacZ}). We show here that these *Mf2*^{lacZ} homozygotes are viable and fertile and have no serious developmental defects, suggesting functional redundancy with other forkhead/winged helix genes. However, up to about 40% of mutants, depending on the genetic background, have renal abnormalities, including hypoplastic kidney and hydroureter. In the long term, *Mf2* mutant mice will provide a useful model to study the interdependent roles of multiple forkhead genes during mammalian development.

MATERIALS AND METHODS

Isolation of *Mf2* genomic DNA and construction of the targeting vector. Two overlapping *Mf2* genomic DNA clones (clones 7 and 10) were isolated from a 129/SvJ mouse genomic λFIXII library (kindly provided by A. Bradley, Baylor College of Medicine) using a probe (0.3 kb) from the 3′ region of the *Mf2* cDNA (44). The single protein coding exon of the *Mf2* genomic sequence encoding amino acids 1 to 492 was confirmed by sequencing. The targeting vector consists of a 6.5-kb 5′ homology region (*Xho*I-*Not*I fragment) and a 0.7-kb 3′ homology region (*Xho*I-*Eco*RI fragment). Part of the coding region (amino acids 92 to 262) was replaced with an IRES-*lacZ*polyA/PGK*neo*^{r} cassette from the NTR-*lacZ* vector (3) and a PGK*neo*bpA-lox-A vector (40) (kindly provided by R. Behringer, M. D. Anderson Cancer Center). This results in the deletion of the entire DNA binding domain. The remaining 5′ region encoding a truncated N-terminal protein sequence is separated from the *lacZ* gene by an in-frame stop codon. For negative selection, a PGK/*tk* cassette was placed outside of the 3′ homology region.

* Corresponding author. Mailing address: Howard Hughes Medical Institute and Department of Cell Biology, Vanderbilt University Medical Center, Nashville, TN 37232-2175. Phone: (615) 343-6418. Fax: (615) 343-2033. E-mail: brigid.hogan@mcmail.vanderbilt.edu.

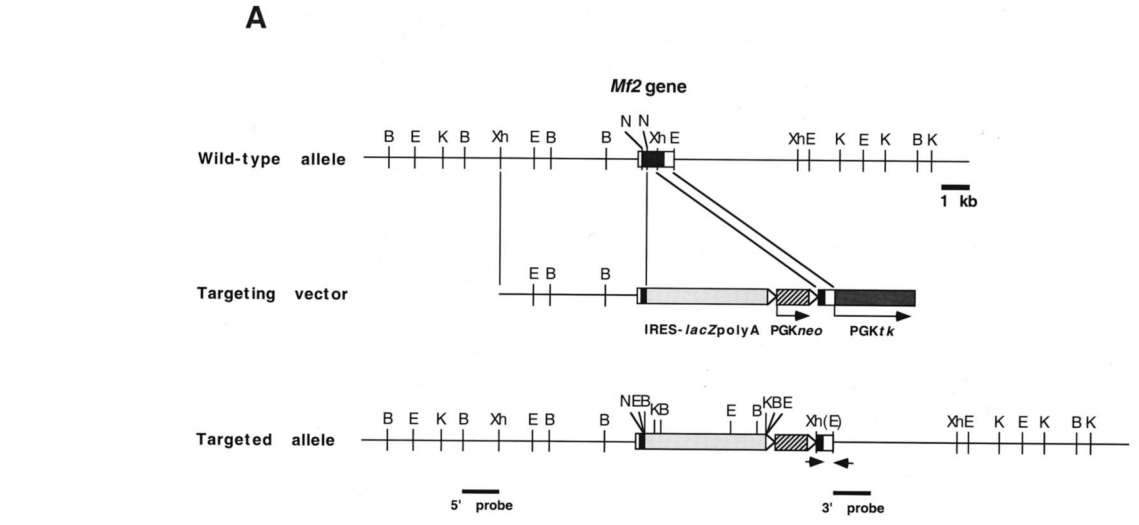

FIG. 1. Generation of homozygous $Mf2^{lacZ}$ mutant mice. (A) The *Mf2* gene (top) contains a single protein-coding exon (black box) flanked by 5′ and 3′ untranslated regions (open boxes). Construction of the targeting vector (middle) is described in Materials and Methods. The targeted $Mf2^{lacZ}$ allele is shown at the bottom. The 5′ and 3′ probes used for screening are indicated by bars. Open arrows indicate the *loxP* sites flanking the PGK*neo* cassette. Arrows represent the primers for PCR screening of targeted ES cells. B, *Bam*HI; E, *Eco*RI; K, *Kpn*I; N, *Not*I; Xh, *Xho*I. Parentheses indicate loss of restriction enzyme sites as a result of construction. (B) Southern blot analysis of a targeted ES cell clone. Using the 5′ probe and *Kpn*I digestion, the wild-type (wt) and targeted (m) loci generate 18- and 8.8-kb bands, respectively. Using the 3′ probe and *Kpn*I digestion, the wild-type and targeted loci generate 18- and 9.3-kb bands, respectively. TL-1 and 9-C indicate the wild-type and targeted ES cells, respectively. (C) PCR analysis of a representative intercross between F_1 mice. The wild-type and targeted alleles give 602- and 570-bp PCR products, respectively. +/+, wild type; +/−, heterozygote, −/−, homozygote.

Isolation of targeted *Mf2* ES cell clones and generation of mouse chimeras. We electroporated 100 μg of *Sal*I-linearized targeting vector into approximately 4×10^7 TL1 ES cells at passage 15 by using a single pulse of 800 V and 3 μF in a Gene Pulser (Bio-Rad). Cells were plated onto irradiated neo^r primary mouse embryo fibroblasts, and selection with G418 and gancyclovir began after 24 and 48 h, respectively. We screened 116 doubly resistant colonies for homologous recombination by PCR using an *Mf2*-5′ primer (5′-TGCATCGCATTGTCTGAGTAGG-3′) and an *Mf2*-3′ primer (5′-CCAAAGCATTCTCTGACTGTGAAGG-3′). PCR-positive clones were confirmed by Southern blotting with 5′ and 3′ external probes. One targeted clone was injected into host (C57BL/6) blastocysts and produced germline chimeras. Chimeras were mated with Black Swiss (Taconic) or C57BL/6 females and maintained by interbreeding on each mixed genetic background. Embryos and mice were genotyped by Southern blotting with a 3′ probe and/or PCR using the specific primers Mf2-1 (5′-AAGTCCTAGAGTTTCAACACCAGGG-3′), Mf2-3 (5′-TTATTCCAAGCGGCTTCGG-3′), and Mf2-5 (5′-TGATGAGGGCGATGTACGAATAAG-3′).

Histological analysis. Embryos were fixed in 4% paraformaldehyde in phosphate-buffered saline, serially dehydrated into 100% methanol, and stored at −20°C. Sections (7 μm) were made by standard procedures. LacZ staining and section in situ hybridization were performed as described previously (25). The following murine cDNAs were used as templates for [α-^{35}S]UTP antisense and sense riboprobes: 0.8-kb *Mf2* and 0.9-kb *Bf2* cDNAs, respectively.

Quantitation of kidney volume. To determine the kidney volume of newborn animals, each kidney was measured along the longitudinal, dorsoventral and mediolateral axes.

RESULTS

Targeted disruption and embryonic expression of *Mf2*. To examine the role of *Mf2* during embryonic development, a null allele was generated by homologous recombination in ES cells. The Mf2 protein is encoded by a single exon, and the sequence covering amino acids 92 to 262 was replaced with an IRES-*lacZ*polyA/PGKneo^r cassette (Fig. 1A), resulting in complete deletion of the DNA binding domain. The inserted *lacZ* allele also allowed the expression of the endogenous gene to be monitored by staining for β-galactosidase activity. The presence of a stop codon before the *lacZ* gene prevented the formation of an Mf2-LacZ fusion protein.

We have previously monitored the expression of *Mf2* by using whole-mount or section in situ hybridization. Using these techniques, *Mf2* is first detected in the paraxial mesoderm of the head and body at 8.5 days postcoitum (dpc) (36, 44). Using the $Mf2^{lacZ}$ allele, we were able to recapitulate the endogenous expression pattern shown previously, providing evidence that the *Mf2* gene was correctly targeted (Fig. 2). In addition, we could examine more precise localization of *Mf2* transcripts using LacZ staining. As shown in Fig. 2A, expression is detected in the somites, branchial arches, and head mesenchyme at 9.5 dpc. Later, as the somites differentiate, *Mf2* expression is restricted to the sclerotome and condensing mesenchyme of the vertebrae (Fig. 2B and C and data not shown). *Mf2* is expressed in a number of other mesodermal-mesenchymal re-

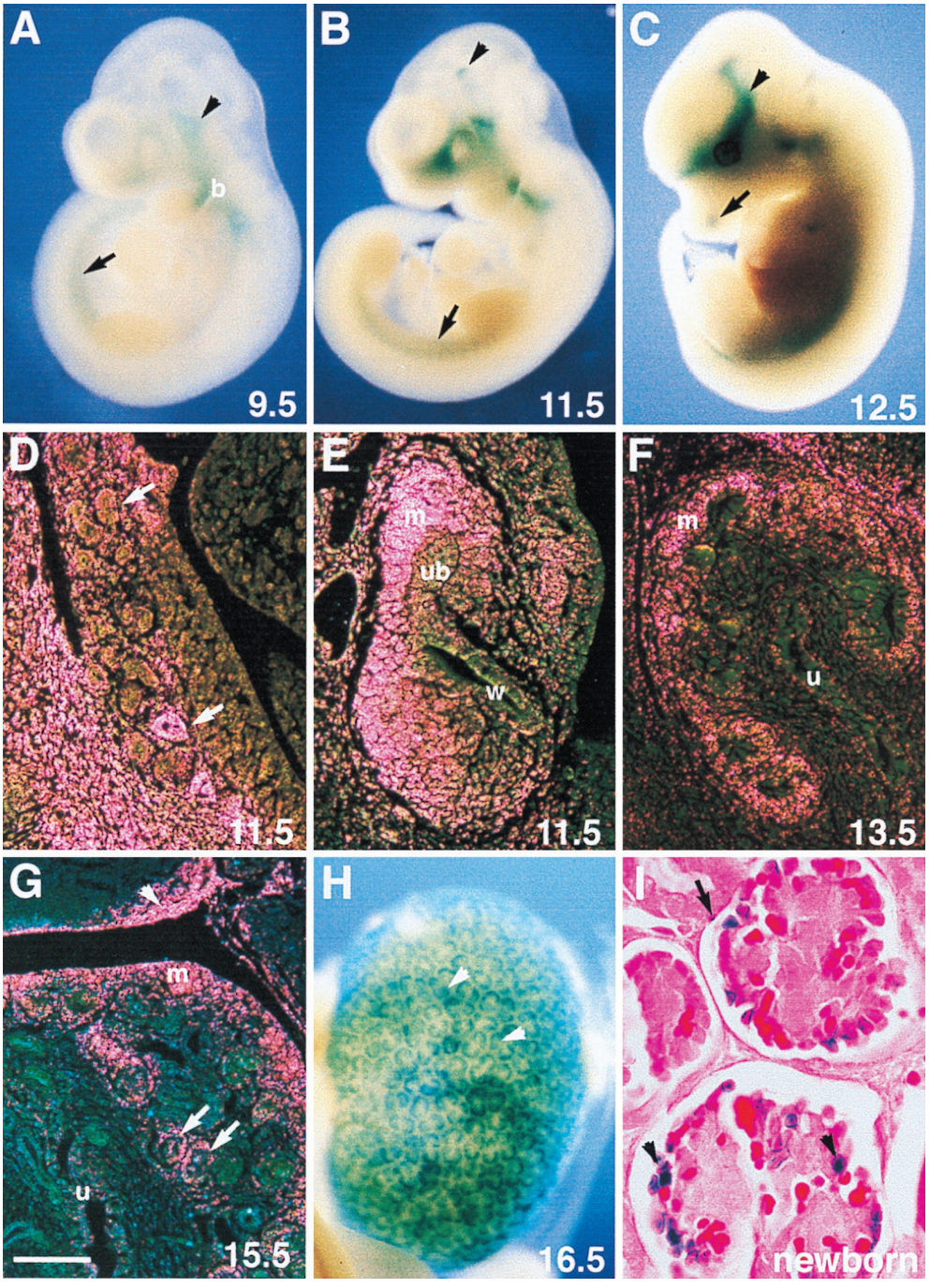

FIG. 2. *Mf2* expression in $Mf2^{lacZ+/-}$ embryos as revealed by LacZ staining. (A) Lateral view of 9.5-dpc embryo. *Mf2* expression is seen in the somites (arrow), cephalic mesoderm (arrowhead), and first and second branchial arches (b). (B) Lateral view of 11.5-dpc embryo with expression in the head mesenchyme including the area around the eye and nasal epithelium, branchial arches, and condensing mesenchyme of the vertebrae (arrow). Expression is also seen in the ventral rostral midbrain and caudal diencephalon (arrowhead). (C) Lateral view of 12.5-dpc embryo showing particularly high expression in the meninges (arrowhead) and nose (arrow). (D to I) Expression of $Mf2^{lacZ}$ in the developing kidney. (D) Parasagittal sections of mesonephros at 11.5 dpc viewed by dark-field illumination; the 5-bromo-4-chloro-3-indolyl-β-D-galactopyranoside (X-Gal) reaction product appears pink. Expression is detected in the epithelium of the mesonephric tubules (arrows) and surrounding mesenchyme. (E) At 11.5 dpc, the strongest expression is in the metanephric mesenchyme surrounding the ureteric bud and only weak signals are detected in the ureteric bud. (F) Strong LacZ staining is observed in the condensing mesenchyme at 13.5 dpc. (G) At 15.5 dpc, *Mf2* expression in the developing kidney is detected in the maturing podocytes (arrows) and condensing mesenchyme in the cortex. Strong $Mf2^{lacZ}$ expression is also seen in the subcapsule of the adrenal gland (arrowhead). (H) Overview of 16.5-dpc kidney. Note the numerous ureteric branches (arrowheads) associated with the LacZ-stained mesenchyme in the cortex. (I) Staining is localized to the podocytes (arrowheads) and Bowman's epithelium (arrow) in the glomeruli of the newborn kidney. m, metanephric mesenchyme; u, ureter; ub, ureteric bud; w, Wolffian duct. Scale bars: D, E, and F, 100 μm; G, 200 μm; I, 25 μm.

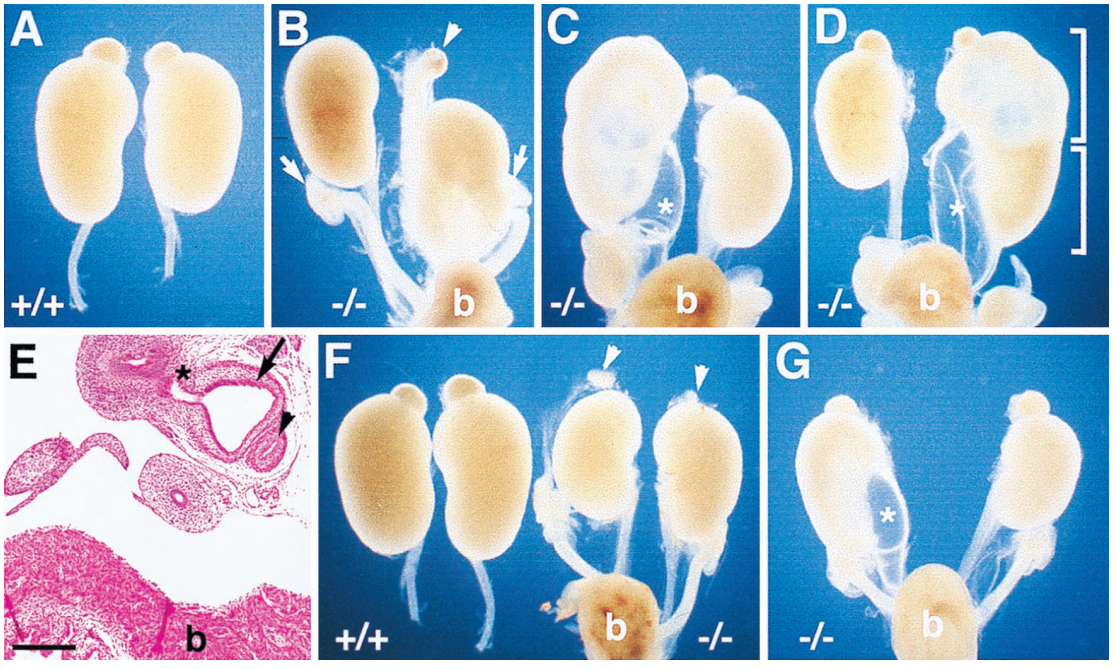

FIG. 3. Kidney and ureter abnormalities in newborn mice homozygous for *Mf2*^{lacZ}. Wild-type (A and F) and mutant (B to G) newborn kidneys are shown. (B) Short hydroureter on the right. Note that the kidney with a short ureter is not attached to the adrenal gland (arrowhead) and both the left and right ovaries (arrows) are located at the same level. (C) Hydronephrosis accompanied by hydroureter (asterisk) on the left. (D) Duplex kidney connected to double ureters on the right showing hydroureter (asterisk). The brackets outline the two conjoined kidneys. (E) Transverse section showing the normal ureter (arrowhead) and the ectopic hydroureter (arrow) abnormally connecting to a derivative (asterisk) of the Wolffian duct. (F) Small kidneys on both the right and left. The adrenal glands (arrowheads) are also small compared with those of the wild type. (G) Hydroureter (asterisk) on the left and small kidney on the right. b, bladder. Scale bar, 200 μm.

gions. In the head of the later embryo, *Mf2* is detected in several tissues, including the tongue, meninges, nasal mesenchyme adjacent to the respiratory epithelium, and vibrissae (Fig. 2B and C and data not shown). In the developing CNS, *Mf2*^{lacZ} is detected in specific regions of the posterior diencephalon-rostral midbrain and its expression continues at least until 16.5 dpc (Fig. 2B and data not shown). LacZ staining is also localized to the tuberal hypothalamus at 11.5 dpc (44 and data not shown).

During development of the kidney, LacZ staining is observed first in the intermediate mesoderm (data not shown) and later in the mesonephric tubules and mesonephric mesenchyme (Fig. 2D). By 11.5 dpc, the ureteric bud has invaded the metanephric blastema and bifurcated. At this stage, strong *Mf2*^{lacZ} expression is seen in the condensing mesenchyme surrounding the tips of the ureter while only a weak signal is present in the stroma and in the Wolffian duct and ureteric epithelium (Fig. 2E). Its expression appears to be similar to that of *Pax2* (8) and also overlaps *Bf2* expression, which is restricted to the stromal cells (16). Two days later, at 13.5 dpc, the ureter has branched several times and LacZ staining is strongly detected in the peripheral condensing mesenchyme of the nephrogenic zone but appears to be weakly expressed in the prospective stromal cells and mesenchyme around the ureter (Fig. 2F and data not shown). From section in situ hybridization using adjacent sections, expression of *Mf2* appears to overlap that of *Bf2* in the stromal cells at 12.5 dpc (data not shown). At 15.5 dpc, the ureter has undergone a significant amount of branching. While differentiated nephrons are observed in the medulla region, new tubules are still being induced from the nephrogenic mesenchyme in the cortex. *Mf2*^{lacZ} expression is detected in the mesenchymal aggregates, as well as in the condensed mesenchyme, and a high level of expression is detected in the developing glomeruli (Fig. 2G). At birth, strong LacZ staining is restricted to nuclei of the podocytes, cells involved in the selective filtration of plasma, and Bowman's epithelium. Its expression also continues in the peripheral mesenchyme of the cortex (Fig. 2I and data not shown).

***Mf2*^{lacZ} homozygotes are viable and fertile.** Homozygous *Mf2*^{lacZ} mutants were generated by intercrossing *Mf2*^{lacZ} heterozygotes (Fig. 1C). They showed the expected Mendelian frequency after weaning (25% of a total of 440 pups on the 129 × Black Swiss genetic background; 20% of a total of 172 pups on the 129 × C57BL/6 genetic background), appeared normal, and were fertile. No obvious skeletal abnormalities were observed in newborn mutants, and the adults apparently behaved normally (data not shown).

***Mf2*^{lacZ} mutants have kidney and ureter abnormalities.** Since *Mf2* is strongly expressed in the developing kidney, we examined the morphology of the kidneys and ureters of newborn mutant mice generated on two different genetic backgrounds (129 × Black Swiss and 129 × C57BL/6) (Fig. 3 and Table 1). On the 129 × Black Swiss genetic background, 23% had hydroureter (fluid-filled ureter) which, in severe cases, was accompanied by hydronephrosis (fluid-filled kidney) (Fig. 3). The prevalence and severity of the kidney phenotype appeared to be significantly increased on the 129 × C57BL/6 genetic background (42%). In addition, on both genetic backgrounds, some mutants had small kidneys or short ureters compared to wild-type mice (Fig. 3 and Table 1). Excluding those with hydronephrosis, the volume of newborn *Mf2* mutant kidneys on the 129 × C57BL/6 genetic background was slightly reduced compared to that of the wild type (+/+, 8.0 ± 0.86 mm^3, $n = 4$; −/−, 6.2 ± 1.4 mm^3, $n = 27$, $P < 0.05$). One *Mf2* mutant on this genetic background had a unilateral duplex kidney

TABLE 1. Kidney and ureter abnormalities in newborn $Mf2^{lacZ}$ mutants[c]

Genotype	No. of mice	No. with:		
		Small kidney(s)[d]	Short ureter(s)	Hydroureter
+/+[a]	5	0	0	0
$Mf2^{lacZ-/-a}$	65	9	3	15 (3)[e]
+/+[b]	3	0	0	0
$Mf2^{lacZ-/-b}$	26	12	0	11 (4)

[a] 129 × Black Swiss genetic background.
[b] 129 × C57BL/6 genetic background.
[c] Bilateral or unilateral traits.
[d] Less than three-fourths of wild-type size.
[e] The values in parentheses are the numbers of kidneys with both hydroureter and hydronephrosis.

connected to double ureters, resulting in hydronephrosis and hydroureter (Fig. 3D). Serial sections revealed that this hydroureter was connected not to the bladder but aberrantly to a derivative (seminal vesicle or vas deferens) of the Wolffian duct (Fig. 3E). Of the kidneys with grossly abnormal phenotypes, 33% were only on the right, 43% were only on the left, and 23% were bilateral.

DISCUSSION

We have generated mice homozygous for a null mutation of *Mf2* and show here that they are viable and fertile, although up to 40% have kidney and ureter abnormalities, including hydroureter, hydronephrosis, small kidneys, and short ureters. From these results, we conclude that in most of the tissues where *Mf2* is expressed there is functional redundancy with other forkhead genes. The kidney phenotype suggests that there are some unique functions of *Mf2* in this organ during development. However, the abnormalities are relatively mild, given the high levels of expression of *Mf2* in this tissue. This discussion will therefore focus on possible roles of *Mf2* in the developing kidney and the possible functional redundancy with other forkhead transcription factors in this organ and other tissues.

Forkhead genes in kidney development. Development of the metanephric kidney depends on a series of reciprocal interactions between the ureteric bud and the metanephric mesenchyme (37). At 10.5 dpc, the metanephric mesenchyme induces the ureteric bud that grows out from the Wolffian duct and invades the metanephric mesenchyme. The ureteric bud subsequently induces the mesenchyme around the tips to condense and undergo a mesenchymal-epithelial transition, ultimately giving rise to nephrons, while the remaining looser peripheral mesenchyme gives rise to stroma. The ureteric bud, in turn, grows and branches to form the ureter, renal pelvis, and collecting system in response to signals from the metanephric mesenchyme. Recent experiments demonstrate that a variety of secreted signaling molecules, transcription factors, and extracellular matrix molecules play important roles in coordinating the proliferation, differentiation, and morphogenesis of the different kidney mesenchymal lineages (for recent reviews, see references 5, 7, and 27). For example, it has been shown that both the induction and branching of the ureter involve glial cell-derived neurotropic factor (GDNF), produced by the metanephric mesenchyme, and its receptors, c-RET and GFRα-1, expressed in the ureteric epithelium (for reviews, see references 34 and 35). Recently, it has also been shown that BMP7 and FGF signaling pathways synergistically regulate nephrogenesis as a result of reciprocal interactions between the condensed mesenchyme and stromal cells (9).

Several forkhead family members have been reported to be expressed during kidney development (16, 20, 25, 30, 31, 32, 42, 44). For example, *Bf2* is expressed specifically in the stromal mesenchymal cells beginning at 11.5 dpc. All *Bf2*-deficient mice die after birth with kidney abnormalities including hypoplastic kidneys (less than one-third of normal size) and small ureters (one-half of normal length) (16). This result provided the first evidence that the stromal cells are required for the differentiation of condensed mesenchyme into tubular epithelium and the growth and branching of the ureter. On the other hand, very little is known about the roles of other forkhead transcription factors during kidney development.

Mf2 encodes a protein with a DNA binding domain only one amino acid different from that of the protein encoded by *Bf2*. We show here that *Mf2* mutant mice are viable, with kidney and ureter abnormalities. However, although in some respects (small size and short ureter) the phenotype of *Mf2* mutants is similar to that of *Bf2* mutants, it is different in being associated with hydroureter and hydronephrosis. Although these abnormalities are quite common in humans, their etiology and underlying molecular mechanisms are still unknown (33). Because of the low penetrance of the phenotype, we have not addressed the primary defects, but several possibilities can be considered tracing back to functions in one or more of the tissues in which *Mf2* is expressed (the intermediate mesoderm, stroma, condensed mesenchyme, and ureters). For example, from clinical data, it has been proposed that hydroureter and hydronephrosis result from accumulation of urine in the ureter and kidney due to the aberrant positioning of the orifice of the ureter in the bladder. This abnormal insertion may trace back to aberrant positioning of the ureteric bud from the Wolffian duct (29). Our finding that one mutant kidney had an extra ureter aberrantly connecting to a derivative of the Wolffian duct (Fig. 3D and E) supports this possibility and suggest that Mf2 in the intermediate mesoderm regulates the differentiation of the metanephric mesenchyme and its expression of *GDNF*, the inducer of the ureteric bud. An alternative, but not mutually exclusive, possibility is that Mf2 plays a role in the apoptosis of the common mesonephric duct, which normally results in the disappearance of the most caudal part of the Wolffian duct when it reaches the cloaca, so that the ureter finally connects to the bladder (38; Y. Miyazaki, K. Oshima, A. Fogo, B. L. M. Hogan, and I. Ichikawa, submitted for publication). Since *Mf2* is expressed in the common mesonephric duct (data not shown), it is possible that the ureter of *Mf2* mutants makes an inappropriate connection to the bladder. This type of analysis must wait until more affected animals are obtained. Hydroureters have been reported in mice with targeted or spontaneous mutations in genes encoding secreted signaling molecules such as Bmp4 (bone morphogenetic protein 4), Bmp5, and Bmp7 (10, 11, 14, 28; Miyazaki et al., submitted). It is therefore possible that Mf2 functions upstream or downstream of some of these genes in the developing kidney.

Some *Mf2* mutant mice have small kidneys and small ureters, abnormalities also seen in *Bf2* mutants. Although the phenotype of *Bf2* mutants is much more severe than that of *Mf2* mutants, *Bf2* mutant mice do not show complete absence of either the kidney or the ureter (16). Since expression of *Mf2* appears to overlap that of *Bf2* in the stromal mesenchyme, it is likely that there is functional redundancy between *Bf2* and *Mf2* in the stroma, a hypothesis that can be tested by generating $Mf2^{lacZ}$ and *Bf2* double mutant mice. Finally, Mf2 may also function in the condensed mesenchyme and affect the branch-

ing and growth of the ureter through the reciprocal interactions that normally occur between the two tissues.

The human homologues of mouse *Mf2* and *Bf2* are *FREAC-9* (*FKHL17*) on chromosome 1p32-p34 and *FREAC-4* (*FKHL8*) on chromosome 5q12-q13, respectively (12, 13). However, no known congenital abnormalities related to the kidney map close to these loci. Like *Mf2* and *Bf2*, both human genes encode proteins with completely identical DNA binding domains but divergent N- and C-terminal regions and are predominantly expressed in the kidney.

Possible functions of Mf2 in other tissues. Except for kidney and ureter abnormalities, *Mf2* mutants have no obvious abnormalities in other tissues in which *Mf2* and *Bf2* are coexpressed, including the tongue, meninges, and mesenchyme of the vibrissae. Besides that of *Bf2*, the expression of several other forkhead genes overlaps that of *Mf2* in the head. For example, *Mfh1* and *Fkh6* are expressed in the dorsal and anterior regions of the tongue (20) and *Mf1* and *Mfh1* are expressed in the meninges (25, 30). In these tissues, *Mf2* mutant mice also have no obvious defects. In brain development, *Mf2* expression is localized to the tuberal hypothalamus, in distinct domains that overlap those of other forkhead genes such as *Fkh4* and *Mf3* (21, 26, 41). *Mf3* mutant mice have CNS defects that relate to its expression in the hypothalamus (26, 41). Although adult *Mf2* mutants appear to behave normally, more detailed behavioral analysis may shed light on the role of *Mf2* in the CNS.

The *Mf2* expression pattern also overlaps those of other forkhead genes, such as *Mf1*, *Mfh1*, and *Mf3* in the paraxial mesoderm, somites, branchial arches, and had mesenchyme (25, 26, 36, 42). *Mf2* mutant mice, however, have no obvious defects in derivatives of these tissues, including the skeleton, suggesting functional redundancy. To test this possibility, we generated $Mf1^{lacZ}$ and $Mf2^{lacZ}$ double homozygous mutants on the 129 × Black Swiss genetic background. The double mutants die at birth with a phenocopy of $Mf1^{lacZ}$ mutants including skeletal defects. Additionally, all double mutants have kidney and ureter abnormalities, including hydroureter and agenesis of the kidney, a phenotype much more severe than that of *Mf2* homozygous mutants (data not shown). Since the majority of *Mf1* mutants on this genetic background have normal kidneys and ureters and *Mf1* and *Mf2* show overlapping expressions during kidney development (T. Kume, K. Deng, and B. L. M. Hogan, unpublished data), these data support the idea of functional redundancy in the developing kidney. Generation of other double homozygous mutant mice with defects in $Mf2^{lacZ}$ and other forkhead genes will shed light on the genetic interrelationship of related forkhead genes during embryonic development.

ACKNOWLEDGMENTS

We thank Yoichi Miyazaki for helpful and stimulating discussions. We also thank Holger Kulessa, Maureen Gannon, and Bettina Wilm for critical reading of the manuscript.

B.L.M.H. is an Investigator of the Howard Hughes Medical Institute.

REFERENCES

1. **Ang, S. L., and J. Rossant.** 1994. HNF-3 beta is essential for node and notochord formation in mouse development. Cell **78:**561–574.
2. **Ang, S. L., A. Wierda, D. Wong, K. A. Stevens, S. Cascio, J. Rossant, and K. S. Zaret.** 1993. The formation and maintenance of the definitive endoderm lineage in the mouse: involvement of HNF3/forkhead proteins. Development **119:**1301–1315.
3. **Bi, W., J. M. Deng, Z. Zhang, R. R. Behringer, and B. de Crombrugghe.** 1999. Sox9 is required for cartilage formation. Nat. Genet. **22:**85–89.
4. **Chen, J., H. J. Knowles, J. L. Hebert, and B. P. Hackett.** 1998. Mutation of the mouse hepatocyte nuclear factor/forkhead homologue 4 gene results in an absence of cilia and random left-right asymmetry. J. Clin. Investig. **102:** 1077–1082.
5. **Davies, J. A., and J. B. Bard.** 1998. The development of the kidney. Curr. Top. Dev. Biol. **39:**245–301.
6. **Dou, C., X. Ye, C. Stewart, E. Lai, and S. C. Li.** 1997. TWH regulates the development of subsets of spinal cord neurons. Neuron **18:**539–551.
7. **Dressler, G. R.** 1999. Kidney development branches out. Dev. Genet. **24:** 189–193.
8. **Dressler, G. R., U. Deutsch, K. Chowdhury, H. O. Nornes, and P. Gruss.** 1990. Pax2, a new murine paired-box-containing gene and its expression in the developing excretory system. Development **109:**787–795.
9. **Dudley, A. T., R. E. Godin, and E. J. Robertson.** 1999. Interaction between FGF and BMP signaling pathways regulates development of metanephric mesenchyme. Genes Dev. **13:**1601–1613.
10. **Dudley, A. T., K. M. Lyons, and E. J. Robertson.** 1995. A requirement for bone morphogenetic protein-7 during development of the mammalian kidney and eye. Genes Dev. **9:**2795–2807.
11. **Dunn, N. R., G. E. Winnier, L. K. Hargett, J. J. Schrick, A. B. Fogo, and B. L. M. Hogan.** 1997. Haploin sufficient phenotypes in Bmp4 heterozygous null mice and modification by mutations in Gli3 and Alx4. Dev. Biol. **188:** 235–247.
12. **Ernstsson, S., R. Betz, S. Lagercrantz, C. Larsson, S. Ericksson, A. Cederberg, P. Carlsson, and Enerback.** 1997. 1997. Cloning and characterization of freac-9 (FKHL171), a novel kidney-expressed human forkhead gene that maps to chromosome 1p32-p34. Genomics **46:**78–85.
13. **Ernstsson, S., S. Pierrou, M. Hulander, A. Cederberg, M. Hellqvist, P. Carlsson, and S. Enerback.** 1996. Characterization of the human forkhead gene FREAC-4. Evidence for regulation by Wilms' tumor suppressor gene (WT-1) and p53. J. Biol. Chem. **271:**21094–21099.
14. **Green, M. C.** 1968. Mechanism of the pleiotropic effects of the short-ear mutant gene in the mouse. J. Exp. Zool. **167:**129–150.
15. **Gruneberg, H.** 1943. Congenital hydrocephalus in the mouse: a case of spurious pleiotropism. J. Genet. **45:**1–21.
16. **Hatini, V., S. O. Huh, D. Herzlinger, V. C. Soares, and E. Lai.** 1996. Essential role of stromal mesenchyme in kidney morphogenesis revealed by targeted disruption of Winged helix transcription factor BF-2. Genes Dev. **10:**1467–1478.
17. **Hiemisch, H., A. P. Monaghan, G. Schutz, and K. H. Kaestner.** 1998. Expression of the mouse Fkh1/Mf1 and Mfh1 genes in late gestation embryos is restricted to mesoderm derivatives. Mech. Dev. **73:**129–132.
18. **Hong, H. K., J. H. Lass, and A. Chakravarti.** 1999. Pleiotropic skeletal and ocular phenotypes of the mouse mutation congenital hydrocephalus (ch/Mf1) arise from a winged helix/forkhead transcription factor gene. Hum. Mol. Genet. **8:**625–637.
19. **Iida, K., H. Koseki, H. Kakinuma, N. Kato, Y. Mizutani-Koseki, H. Ohuchi, H. Yoshioka, S. Noji, K. Kawamura, Y. Kataoka, F. Ueno, M. Taniguchi, N. Yoshida, T. Sugiyama, and N. Miura.** 1997. Essential roles of the winged helix transcription factor MFH-1 in aortic arch patterning and skeletogenesis. Development **124:**4627–4638.
20. **Kaestner, K. H., S. C. Bleckmann, A. P. Monaghan, J. Schlondorff, A. Mincheva, P. Lichter, and G. Schutz.** 1996. Clustered arrangement of winged helix genes fkh-6 and MFH-1: possible implications for mesoderm development. Development **122:**1751–1758.
21. **Kaestner, K. H., G. Schutz, and A. P. Monaghan.** 1996. Expression of the winged helix genes fkh-4 and fkh-5 defines domains in the central nervous system. Mech. Dev. **55:**221–230.
22. **Kaestner, K. H., D. G. Silberg, P. G. Traber, and G. Schutz.** 1997. The mesenchymal winged helix transcription factor Fkh6 is required for the control of gastrointestinal proliferation and differentiation. Genes Dev. **11:** 1583–1595.
23. **Kaufmann, E., and W. Knochel.** 1996. Five years on the wings of fork head. Mech. Dev. **57:**3–20.
24. **Kidson, S. H., T. Kume, K. Deng, V. Winfrey, and B. L. M. Hogan.** 1999. The forkhead/winged-helix gene, Mf1, is necessary for the normal development of the cornea and formation of the anterior chamber in the mouse eye. Dev. Biol. **211:**306–322.
25. **Kume, T., K. Y. Deng, V. Winfrey, D. B. Gould, M. A. Walter, and B. L. M. Hogan.** 1998. The forkhead/winged helix gene Mf1 is disrupted in the pleiotropic mouse mutation congenital hydrocephalus. Cell **93:**985–996.
26. **Labosky, P. A., G. E. Winnier, T. L. Jetton, L. Hargett, A. K. Ryan, M. G. Rosenfeld, A. F. Parlow, and B. L. M. Hogan.** 1997. The winged helix gene, Mf3, is required for normal development of the diencephalon and midbrain, postnatal growth and the milk-ejection reflex. Development **124:**1263–1274.
27. **Lechner, M. S., and G. R. Dressler.** 1997. The molecular basis of embryonic kidney development. Mech. Dev. **62:**105–120.
28. **Luo, G., C. Hofmann, A. L. Bronckers, M. Sohocki, A. Bradley, and G. Karsenty.** 1995. BMP-7 is an inducer of nephrogenesis, and is also required for eye development and skeletal patterning. Genes Dev. **9:**2808–2820.
29. **Mackie, G. G., and F. D. Stephens.** 1975. Duplex kidneys: a correlation of renal dysplasia with position of the ureteral orifice. J. Urol. **114:**274–280.
30. **Miura, N., A. Wanaka, M. Tohyama, and K. Tanaka.** 1993. MFH-1, a new member of the fork head domain family, is expressed in developing mesenchyme. FEBS Lett. **326:**171–176.
31. **Overdier, D. G., H. Ye, R. S. Peterson, D. E. Clevidence, and R. H. Costa.**

1997. The winged helix transcriptional activator HFH-3 is expressed in the distal tubules of embryonic and adult mouse kidney. J. Biol. Chem. **272:** 13725–13730.
32. **Pelletier, G. J., S. L. Brody, H. Liapis, R. A. White, and B. P. Hackett.** 1998. A human forkhead/winged-helix transcription factor expressed in developing pulmonary and renal epithelium. Am. J. Physiol. **274:**L351–L359.
33. **Pope, J. C. T., J. W. Brock 3rd, M. C. Adams, F. D. Stephens, and I. Ichikawa.** 1999. How they begin and how they end: classic and new theories for the development and deterioration of congenital anomalies of the kidney and urinary tract, CAKUT. J. Am. Soc. Nephrol. **10:**2018–2028.
34. **Rosenthal, A.** 1999. The GDNF protein family: gene ablation studies reveal what they really do and how. Neuron **22:**201–203.
35. **Sariola, H., and K. Sainio.** 1997. The tip-top branching ureter. Curr. Opin. Cell Biol. **9:**877–884.
36. **Sasaki, H., and B. L. M. Hogan.** 1993. Differential expression of multiple fork head related genes during gastrulation and axial pattern formation in the mouse embryo. Development **118:**47–59.
37. **Saxen, L.** 1987. Organogenesis of the kidney. Cambridge University Press, Cambridge, England.
38. **Stephens, F. D., and J. M. Huston.** 1996. Congenital anomalies of the urinary and genital tracts. ISIS Medical Media, Oxford, England.
39. **Swiderski, R. E., R. S. Reiter, D. Y. Nishimura, W. L. Alward, J. W. Kalenak, C. S. Searby, E. M. Stone, V. C. Sheffield, and J. J. Lin.** 1999. Expression of the Mf1 gene in developing mouse hearts: implication in the development of human congenital heart defects. Dev. Dyn. **216:**16–27.
40. **Wakamiya, M., E. A. Lindsay, J. A. Rivera-Perez, A. Baldini, and R. R. Behringer.** 1998. Functional analysis of Gscl in the pathogenesis of the DiGeorge and velocardiofacial syndromes. Hum. Mol. Genet. **7:**1835–1840.
41. **Wehr, R., A. Mansouri, T. de Maeyer, and P. Gruss.** 1997. Fkh5-deficient mice show dysgenesis in the caudal midbrain and hypothalamic mammillary body. Development **124:**4447–4456.
42. **Winnier, G. E., L. Hargett, and B. L. M. Hogan.** 1997. The winged helix transcription factor MFH1 is required for proliferation and patterning of paraxial mesoderm in the mouse embryo. Genes Dev. **11:**926–940.
43. **Winnier, G. E., T. Kume, K. Deng, R. Rogers, J. Bundy, C. Raines, M. A. Walter, B. L. M. Hogan, and S. J. Conway.** 1999. Roles for the winged helix transcription factors MF1 and MFH1 in cardiovascular development revealed by nonallelic noncomplementation of null alleles. Dev. Biol. **213:**418–431.
44. **Wu, S. C., J. Grindley, G. E. Winnier, L. Hargett, and B. L. M. Hogan.** 1998. Mouse mesenchyme forkhead 2 (Mf2): expression, DNA binding and induction by sonic hedgehog during somitogenesis. Mech. Dev. **70:**3–13.
45. **Xuan, S., C. A. Baptista, G. Balas, W. Tao, V. C. Soares, and E. Lai.** 1995. Winged helix transcription factor BF-1 is essential for the development of the cerebral hemispheres. Neuron **14:**1141–1152.